Solid State Ionics 319 (2018) 223–227

Contents lists available at ScienceDirect

Solid State Ionics

journal homepage: www.elsevier.com/locate/ssi

Preparation of lanthanum silicate electrolyte with high conductivity and high chemical stability

Atsushi Mineshige[a,*], Hikaru Hayakawa[a], Takuma Nishimoto[a], Akie Heguri[a], Tetsuo Yazawa[a], Yuki Takayama[b,c], Yasushi Kagoshima[b,c], Hidekazu Takano[d], Shingo Takeda[e], Junji Matsui[c]

[a] Department of Applied Chemistry, Graduate School of Engineering, University of Hyogo, Himeji, Hyogo 671-2201, Japan
[b] Graduate School of Material Science, University of Hyogo, 3-2-1, Kouto, Kamigori, Ako, Hyogo 678-1297, Japan
[c] Synchrotron Radiation Nanotechnology Center, University of Hyogo, 1-490-2, Kouto, Shingu, Tatsuno, Hyogo 679-5165, Japan
[d] Institute of Multidisciplinary Research for Advanced Materials, Tohoku University, 2-1-1, Katahira, Aoba-ku, Sendai, Miyagi 980-8577, Japan
[e] SPring-8 Service Co., Ltd., 1-20-5, Kouto, Shingu, Tatsuno, Hyogo 679-5165, Japan

ARTICLE INFO

Keywords:
Apatite
Lanthanum silicate
Synchrotron radiation microbeam

ABSTRACT

Effects of dopant content and synthesis temperature on phase relations and conducting behavior of lanthanum silicate, $La_{9.33+x}Si_6O_{26+1.5x}$ (LSO) electrolytes were investigated. The La-excess-type Fe-doped LSO, $La_{10}(Si_{5.5}Fe_{0.5})O_{26.75}$ synthesized at 1973 K showed lower grain boundary as well as grain interior resistances, and then, had high total conductivity (6.9×10^{-3} S cm^{-1} at 873 K and 3.6×10^{-5} S cm^{-1} at 573 K). In addition, the chemical instability owing to a high lanthanum activity in the La-excess-type LSO ($x = 0.67$) specimen could be eliminated by incorporating iron into the specimen. The synchrotron radiation microbeam X-ray diffraction technique revealed that this specimen contains a small amount of new secondary phase, which differs from the situation found in a highly conductive but chemically unstable Al-doped LSO specimen with the same x value and the same synthesis temperature.

1. Introduction

Apatite-type lanthanum silicate ($La_{9.33+x}Si_6O_{26+1.5x}$, LSO) found by Nakayama [1,2], has attracted much attention as oxide ion (O^{2-}) conductors used in intermediate-temperature as well as high-temperature operating electrochemical devices. LSO is oxygen-excess-type solid electrolyte and then, exhibits lower activation energy for ionic conduction (ca. 0.6 eV), which is a good feature for the intermediate-temperature operation (below ca. 873 K) of the high-temperature operating devices. Recently, it has been recognized that there are some problems to be solved for the application of LSO as electrolyte materials in a practical use, such as chemical instability towards water in the ambient air [3,4], or diffusion of silicon to electrode materials across the electrode/electrolyte interface [5–7]. In addition, a firing temperature for the sample synthesis is also important, and very high firing temperature (e.g. 1973 K) is needed for getting high conductivity. Preferential orientation is another key challenge to be required for further enhancement in conductivity of LSO because of the existence of the fast ion conducting channel along its c axis [8–10].

To obtain high ionic conductivity using an LSO polycrystalline specimen, introduction of additional lanthanum into the LSO crystal lattice is effective, and in fact, the total electrical conductivity, σ (*tot*), of this material was enhanced with an increase in x [11,12]. This is because the excess oxide ions ($1.5x$) as oxygen interstitials, which are thought to be ionic carrier of this kind of materials, could be introduced into this material with an increase in x. On the other hand, it becomes chemically unstable in the case with larger x value ($x >$ ca. 0.5). In our previous study [3], the chemical composition was optimized as $La_{10}(Si_{5.8}Al_{0.2})O_{26.9}$, which exhibits the highest σ (*tot*) among Al-doped LSO electrolytes. However, the optimum specimen synthesized at 1973 K suffered from sample degradation due to its chemical instability. To solve this problem, in our previous study [3,4,13], a small amount of iron addition into the optimum composition, $La_{10}(Si_{5.8}Al_{0.2})O_{26.9}$, was studied, and its transport properties were examined by evaluating oxygen tracer diffusion coefficient and partial electronic conductivity in addition to the DC conductivity measurement. It was found that the conductivity degradation could be mitigated by iron addition, and the ion transport number was still almost unity in spite of the Fe addition. However, the mechanism of the stabilization with iron addition has not been clarified yet.

In the present study, we prepared Fe-doped LSO, and their phase relations, conducting behavior, and chemical stability were

* Corresponding author at: 2167 Shosha, Himeji, Hyogo 671-2201, Japan.
E-mail address: mine@eng.u-hyogo.ac.jp (A. Mineshige).

https://doi.org/10.1016/j.ssi.2018.02.002
Received 30 September 2017; Received in revised form 10 January 2018; Accepted 2 February 2018

investigated compared with the Al-doped LSO system. It has been reported by Kharton et al. [14] that Fe-doping into $La_{10}Si_6O_{27}$ resulted in the enhancement in the conductivity of LSO as seen in the Al-doping system. In addition, they [14] reported that Fe^{3+} state was stable in the $La_{10}(Si_{6-y}Fe_y)O_{27-0.5y}$ system, and ionic conduction remains dominant under solid oxide fuel cell (SOFC) operation conditions. Hence, we prepared the Fe-doped LSO with high La content ($x = 0.67$), and studied the effect of the dopant content (y) and synthesis temperature on its properties. In addition, to elucidate a contribution of the grain boundary on the ion transport property, AC impedance measurements were performed. Furthermore, the synchrotron radiation microbeam X-ray technique was employed to investigate the local precipitation of secondary phase, and the relationship between their phase relations and its properties was discussed.

2. Experimental

2.1. Preparation of Fe-doped LSO

Fe-doped LSO specimens, which weighted composition was $La_{10}(Si_{6-y}Fe_y)O_{27-0.5y}$ ($y = 0.2, 0.5, 1.0$) were synthesized via a conventional solid-state reaction route from a mixture of raw powders of La_2O_3 (99.99% purity, Kojundo Chemical Lab. Co., Ltd.), SiO_2 (99.9% purity, Kojundo Chemical Lab. Co., Ltd.), and Fe_2O_3 (99% purity, Kanto Chemical Co., Inc.). Starting powders were mixed in ethanol for 3 h with a planetary ball mill rotated at a speed of 300 rpm, and then calcined at 1673 K for 10 h in air. After grinding, powders were pressed into a disc at 57 MPa, followed by sintering at 1973 K for 10 h in air. Firing temperatures (T_f) for the sample sintering of 1873 and 2023 K were also studied in case of $y = 0.5$. The heating and cooling rates were 200 K/h.

2.2. Characterization of Fe-doped LSO

The specimens obtained were characterized by X-ray diffraction (XRD, Ultima IV, Rigaku Corp.). Sample density was evaluated by using Archimedes method. Scanning electron microscopy with energy dispersive X-ray spectroscopy (SEM-EDX, JSM-7001F, JEOL Ltd.) was carried out to investigate microstructure and element analyses of specimens. Four-probe DC conductivity measurements using a galvanostat (HA-151, Hokuto Denko Corp.) and an electrometer (R6452E, Advantest Corp.), and AC impedance measurements using Frequency Response Analyzer (1255B, Solartron Analytical) were performed at temperatures ranged between 573 and 1073 K in ambient air. In order to understand the contribution of a grain boundary resistance, impedance Nyquist plot was fitted using an equivalent circuit consisting grain interior (g_i) and grain boundary (g_b) resistances and their capacitances, expressed by the constant phase elements, in series. The ZPlot software (Scribner Associates, Inc.) was used for this purpose.

2.3. Determination of local precipitation in Fe-doped LSO

To investigate the phase relations of the Fe-doped LSO in detail, synchrotron radiation microbeam X-ray diffraction (SR-μXRD) was measured at the Hyogo ID beamline BL24XU of SPring-8, Japan, using Fresnel zone-plate optics for focusing synchrotron radiation X-ray down to the size of the micrometer range [15–17]. The incident beam of $\lambda = 0.0826$ nm ($E = 15.0$ keV) was focused to 0.7 μm (V) × 1.0 μm (H) in full width at half maximum intensity with a photon flux of $\sim 10^9$ photons/s. The thickness of the specimens was adjusted to 50 μm to avoid a self-absorption. To collect X-ray diffraction spots, a flat panel detector (C9728DK-10, Hamamatsu Photonics K. K.) was used. At first, measurements were carried out by moving the sample in the focal plane in two directions (2–10 μm step). During the measurements, a fluorescence spectrum from the sample was also collected using a silicon drift detector (SDD, XR-100SDD, AMPTECK, Inc.) aiming at detection of a concentrated region of iron. Then, for the selected area containing iron-concentrated region, a detailed two-dimensional measurement was done with 1 μm step. By integrating the intensity of each diffraction spot in azimuthal direction and summing the integrated profiles over the selected area, diffraction profile of the selected area was obtained.

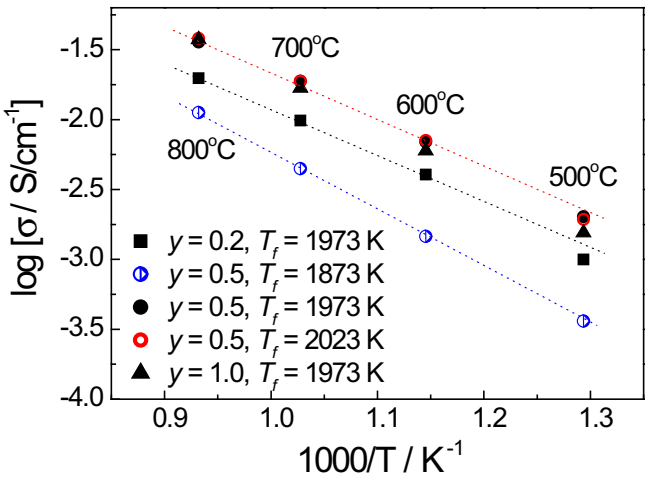

Fig. 1. Total electrical conductivity, $\sigma(tot)$ of $La_{10}(Si_{6-y}Fe_y)O_{27-0.5y}$ ($y = 0.2, 0.5, 1.0$) as a function of temperature. For $y = 0.5$, an effect of T_f was also examined. Each dotted line shown is just a guide to the eye.

3. Results and discussion

Fig. 1 shows temperature dependency of the total electrical conductivity, $\sigma(tot)$ for $La_{10}(Si_{6-y}Fe_y)O_{27-0.5y}$ ($y = 0.2, 0.5, 1.0$) obtained by the four-probe DC conductivity measurements. As shown in this graph, $\sigma(tot)$ tended to increase with increases in y and T_f. In Fe-doped LSO series studied, $La_{10}(Si_{5.5}Fe_{0.5})O_{26.75}$ with $T_f = 1973$ K showed the highest conductivity (3.6×10^{-2} S cm^{-1} at 1073 K, and 6.9×10^{-3} S cm^{-1} at 873 K). These values were higher than those described in the above mentioned literature (2.5×10^{-2} S cm^{-1} at 1073 K, and 4.0×10^{-3} S cm^{-1} at 873 K, respectively) for $La_{10}(Si_5Fe)O_{26.5}$ specimen with $T_f = 1773$ K [14]. In our previous report [18], the effect of Al-doping into LSO on σ (tot) was investigated, and it was found that a slight Al-doping increased σ (tot). A similar trend was found for the case in the Mg-doping system [19]. We have discussed about the reason for the increase in σ (tot) with Al-doping [20,21], and it was suggested that an oxygen vacancy or a weakly-bonded oxygen atom was created in an SiO_4 tetrahedral unit by introducing a lower valent cation into the Si-site. This may contribute an alternative conducting path in the lattice, resulting in enhancement of the overall conductivity. A similar mechanism might occur in the Fe-doped system. On a closer look on Fig. 1, there seems to be an inflection point for each plot at around 873 K. This suggests that grain boundary resistance became dominant in the intermediate-temperature region. This will be discussed later.

Regarding chemical stability of the 1973 K- and 1873 K-fired $La_{10}(Si_{5.5}Fe_{0.5})O_{26.75}$ specimens, no troubles were found when placed in ambient air. Although the 2023 K-fired specimen with $y = 0.5$ showed a similar high conductivity as the 1973 K-fired one, it was chemically unstable and broke down into fine powders in few days. Hence, it was found that a $La_{10}(Si_{5.5}Fe_{0.5})O_{26.75}$ specimen with $T_f = 1973$ K is suitable for the application. To understand the reason why chemical stability relies on T_f, phase relations should be evaluated.

Fig. 2 shows XRD patterns of the Fe-doped system ($y = 0.5$) with different T_f. In case of $T_f = 1973$ K, the specimen was found to be an almost single phase of the apatite-type LSO. However, the secondary phase was observed in addition to the LSO phase in case of $T_f = 1873$ K and 2023 K. A small amount of La_2SiO_5 and hexagonal La_2O_3 (h-La_2O_3) phases were observed for the 1873 K- and 2023 K-fired specimens,